Organic–Inorganic Hybrid Composites

DOI: 10.1002/anie.201409653

Threading Chalcogenide Layers with Polymer Chains**

*Wei-Wei Xiong, Jianwei Miao, Kaiqi Ye, Yue Wang, Bin Liu, and Qichun Zhang**

Abstract: *Inserting polymers into a crystalline inorganic matrix to understand the structure, position, and the structure–property relationships of the resulting composites is important for designing new inorganic-organic materials and tuning their properties. Single crystals of polymer-chalcogenide composites were successfully prepared by trapping polyethyleneglycol within a selenidostannate matrix under surfactant-thermal conditions. This work might provide a new strategy for preparing novel crystalline polymer-inorganic composites through encapsulating polymer chains within inorganic matrices.*

Encapsulation of polymer chains into crystalline inorganic materials has attracted considerable interest because these composites not only provide a fundamental understanding of structure–property relationships but also have potential technological applications.[1] To date, three extensively studied porous matrices [zeolites, metal–organic frameworks (MOFs), and mesoporous silica (e.g. MCM-41)][2] have been demonstrated as hosts to control the polymerization of monomers within their regular channels. The as-formed polymer chains possess high stereoregularity, which plays an important role in determining the mechanical and electronic properties of the resulting nanocomposites.[3] Besides these three-dimensional porous materials, two-dimensional layered structures such as clays, FeOCl, V_2O_5, and MoO_3, have also been used as hosts to intercalate guest monomers for the polymerization between the layers.[4] Most of these polymer/inorganic nanocomposites were prepared through the adsorption of monomers into a matrix and subsequent polymerization. However, this synthetic strategy is unlikely to obtain high quality single crystals for precisely understanding the structure of the polymers, and the position and the interaction between polymer chains and hosts, because it is very challenging to maintain the as-prepared polymers and inorganic frameworks after long-range ordering simultaneously. Thus, multiple characterization methods (e.g. IR, NMR spectroscopy, SEM, and molecular dynamics calculations) are required to understand the nature of the nanocomposites.[5] Since single-crystal structure analysis could directly provide more detailed and precise structural information of a nanocomposite, it is highly desirable to develop a new method to prepare high-quality single crystals of polymer/inorganic nanocomposites for structure solving.

Crystalline chalcogenides have been considered as one of most important inorganic materials in solid-state chemistry because of their diverse structures and unique properties.[6] Although numerous meso- and microporous chalcogenides with uniform channels have been reported in the past decades,[7] employing chalcogenide frameworks as hosts to encapsulate polymers has been less explored. Two-dimensional MoS_2 has been demonstrated to intercalate polymers,[8] however, trying to grow single crystals of these nanocomposites under current methods are impractical. Thus, developing alternative synthetic strategy to achieve single crystals of polymer/chalcogenides is necessary.

Recently, our group demonstrated that surfactants can be employed as reaction media to prepare novel crystalline inorganic complexes.[9] Continuing with this research, we believe that this reaction system could be a promising media to encapsulate polymer chains within inorganic matrices because surfactants have good solubility of polymers as a surfactant itself is a polymer. In this study, we firstly report the single-crystal growth of the polymer/chalcogenide complex $[DBNH]_2[Sn_3Se_7]\cdot PEG$ (**1**) (DBN = 1,5-diazabicyclo-[4.3.0]non-5-ene; PEG = polyethyleneglycol) under surfactant-thermal conditions. The single-crystal structural analysis reveals that the PEG chains are threaded through the nanochannels of the two-dimensional honeycomb $[Sn_3Se_7]_n^{2n-}$ layers, and is quite different from the previously reported nanocomposites based on a two-dimensional inorganic layer, where polymers are located between the layers.[4] Subsequent investigation suggests that the synthesis of **1** can be thermodynamically controlled, since an isostructural chalcogenide without PEG chains, $[DBNH]_3[NH_4][Sn_6Se_{14}]$ (**3**), has been synthesized at a higher reaction temperature under the same reaction conditions. In addition, photoelectrochemical studies indicate that **1** exhibits n-type semiconductor behavior under visible-light illumination ($\lambda >$ 400 nm).

Orange block crystals of **1** were synthesized by reacting Sn and Se in the mixed solution of DBN, H_2O, ethylene glycol, and PEG-400 at 120 °C for six days. Single-crystal X-ray analysis revealed that **1** crystallizes in the monoclinic space group *C*2/*c*. As shown in Figure 1, the structure consists of two-dimensional anionic $[Sn_3Se_7]_n^{2n-}$ layers, $[DBNH]^+$ cat-

[*] Dr. W.-W. Xiong, Prof. Dr. Q.-C. Zhang
School of Materials Science and Engineering
Nanyang Technological University
Singapore 639798 (Singapore)
E-mail: qczhang@ntu.edu.sg
J.-W. Miao, Prof. Dr. B. Liu
School of Chemical & Biomedical Engineering
Nanyang Technological University, Singapore 637459 (Singapore)
Dr. K.-Q. Ye, Prof. Dr. Y. Wang
State Key Laboratory of Supramolecular Structure and Materials
College of Chemistry, Jilin University
Changchun 130012 (P.R. China)

[**] Q.Z. acknowledges the financial support from AcRF Tier 1 (RG 16/12), Tier 2 (ARC 20/12 and ARC 2/13) from MOE, and the CREATE program (Nanomaterials for Energy and Water Management) from NRF, Singapore.

Supporting information for this article is available on the WWW under http://dx.doi.org/10.1002/anie.201409653.

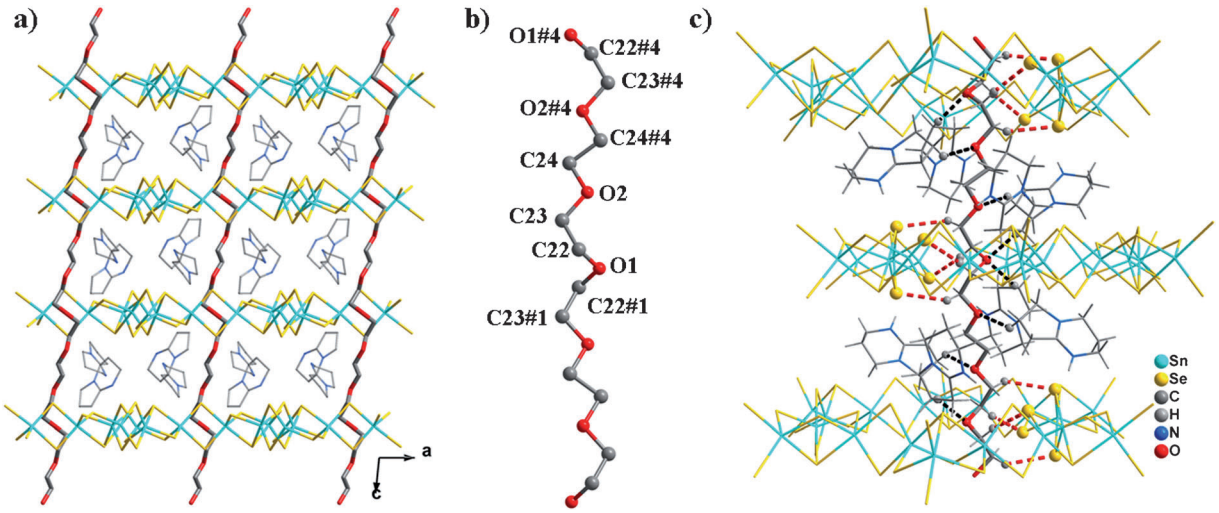

Figure 1. a) The extended PEG chains thread through the nanochannels of the honeycomb $[Sn_3Se_7]_n^{2n-}$ layers along the *c* axis, and the hydrogen atoms are omitted for clarity. b) The conformation of one single PEG chain in **1**. c) The oxygen atoms of the PEG chain interact with $DBNH^+$ cations through C–H···O hydrogen bonds (black dashed lines), while C22–H22 and C23–H23 groups of the PEG chain interact with Se^{2-} ions from inorganic $[Sn_3Se_7]_n^{2n-}$ layers through C–H···Se hydrogen bonds (gray dashed lines). #1 $-x, y, -z+1/2$; #4 $-x, -y+1, -z+1$.

ions, and PEG chains. In the structure of **1**, Sn^{4+} coordinates with five Se^{2-} ions to generate a $[SnSe_5]$ trigonal-bipyramid, and three such units further connect to each other through sharing the edge Se^{2-} ions to form the $[Sn_3Se_{10}]$ block. The adjacent $[Sn_3Se_{10}]$ blocks alternately link together to form a $[Sn_6Se_{16}]$ chain along the *b* axis. Then, these chains share the edge Se^{2-} ions along the *a* axis to produce the honeycomb $[Sn_3Se_7]_n^{2n-}$ layer,[10] which contains regular windows constructed by six edge-sharing $[Sn_3Se_{10}]$ blocks. The honeycomb $[Sn_3Se_7]_n^{2n-}$ layers pack along the *c* axis, and a series of nanochannels are generated by the orderly arrangement of windows. The PEG chains are inserted within nanochannels of the honeycomb $[Sn_3Se_7]_n^{2n-}$ layers along *c* axis (Figure 1 a). The $DBNH^+$ cations act as charge-balance species and are located between the layers. Different from traditional polymer/inorganic nanocomposites based on the utilization of layered inorganic materials, such as FeOCl, V_2O_5, MoO_3, and MoS_2,[4,8] the PEG chains in **1** thread through the nanochannels of the $[Sn_3Se_7]_n^{2n-}$ layers, which might be attributed to the honeycomb structure and flexible arrangements of $[Sn_3Se_7]_n^{2n-}$ layers.

The single-crystal X-ray analysis of **1** can also provide the chance to investigate the conformation of PEG chains in **1**, and the interactions between the PEG chains and the inorganic $[Sn_3Se_7]_n^{2n-}$ layers or $DBNH^+$ cations. Three ethylene oxide units are needed to represent the conformation of the PEG chain, which contains *trans* (*T*) and *gauche* (*G*) conformations. The torsion angles of the PEG chain are listed in Table 1. As shown in Figure 1 b, when counting from the O1 atom, the conformation of PEG chains can be noted as *GTTTTTGGG*. In the nanochannels constructed by the arrangement of the $[Sn_3Se_7]_n^{2n-}$ layers and $DBNH^+$ cations, PEG chains interact with $[Sn_3Se_7]_n^{2n-}$ layers and $DBNH^+$ cations through various hydrogen bonds, which are summarized in Table 2. As shown in Figure 1 c, the oxygen atoms of the PEG chain interact with $DBNH^+$ cations through C–H···O hydrogen bonds (black dashed line), while the C22–H22 and C23–H23 groups of PEG chain interact with Se^{2-} ions from inorganic $[Sn_3Se_7]_n^{2n-}$ layers through C–H···Se hydrogen bonds (gray dashed line). It is noticeable that the various hydrogen bonds between PEG chains and inorganic hosts have a contribution to confining the conformation of the PEG chains within the nanochannels.

Table 1: Torsion angles (°) for the PEG chain.[a]

O(1)-C(22)-C(23)-O(2)	−76(2)
C(22)-C(23)-O(2)-C(24)	180(2)
C(24)#4-C(24)-O(2)-C(23)	165(3)
C(23)-C(22)-O(1)-C(22)#1	−71.0(14)

[a] Symmetry codes: #1 $-x, y, -z+1/2$; #4 $-x, -y+1, -z+1$.

Table 2: Hydrogen bonds for $[DBNH]_2[Sn_3Se_7]$·PEG (**1**).[a]

D-H···A	d(H···A) [Å]	d(D···A) [Å]	< (DHA) [°]
C(22)-H(22B)···Se(7)	2.83	3.77(2)	163.7
C(23)-H(23 A)···Se(6)#1	2.96	3.58(2)	122.9
C(11)-H(11A)···O(1)	2.44	3.22(2)	136.7
C(14)-H(14B)···O(2)#5	2.59	3.36(4)	136.9
N(2)-H(2C)···Se(5)	2.89	3.633(13)	146.4
N(4)-H(4C)···Se(3)	2.64	3.451(10)	157.3

[a] Symmetry codes: #1 $-x, y, -z+1/2$; #5 $x, -y+1, z-1/2$.

Black plate crystals of **2** were also obtained in the synthesis of **1**. Single-crystal X-ray analysis indicated that **2** belongs to the monoclinic space group $P2_1/c$. Its structure features a two-dimensional anionic $[Sn_4Se_8(Se_6)(Se_2)_{1/2}]_n^{3n-}$ layer with $DBNH^+$ cations between the layers. In the structure of **2**, one kind of Sn^{4+} ion coordinates with five Se^{2-} ions to generate a $[SnSe_5]$ trigonal-bipyramid, and subsequently acts as a primary building unit in the construction of the $[Sn_6Se_{16}]$ chain, which is also formed in the structure of **1**. The other kind of Sn^{4+} ion also adopts trigonal-bipyramidal coordination geometry by linking to two Se^{2-} ions, one Se_2^{2-} ion, and one Se_6^{2-} ion to form a $[SnSe_2(Se_2)$-

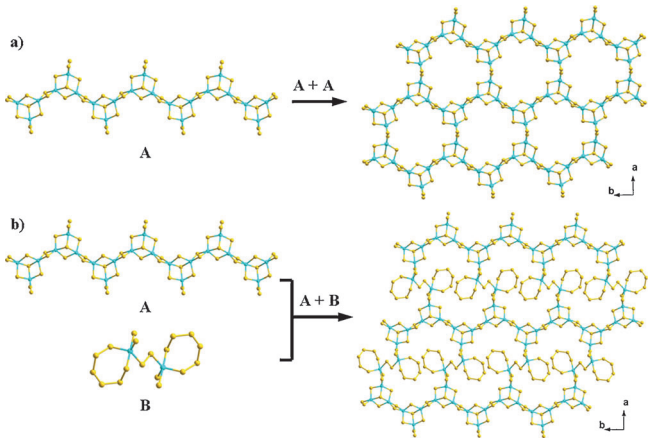

Figure 2. a) The $[Sn_3Se_7]_n^{2n-}$ layer in **1** is built up by the condensation of $[Sn_6Se_{16}]$ chains along the *a* axis. b) The $[Sn_4Se_8(Se_6)(Se_2)_{1/2}]_n^{3n-}$ layer in **2** is constructed by alternating $[Sn_6Se_{16}]$ chains and $[Sn_2Se_4(Se_2)(Se_6)_2]$ dimers.

$(Se_6)]$ unit. Two such units connect to each other through the Se_2^{2-} ion to generate a $[Sn_2Se_4(Se_2)(Se_6)_2]$ dimer. The $[Sn_6Se_{16}]$ chains are bridged by $[Sn_2Se_4(Se_2)(Se_6)_2]$ dimers through edge-sharing Se^{2-} ions along the *a* axis, and result in the formation of the two-dimensional anionic $[Sn_4Se_8(Se_6)(Se_2)_{1/2}]_n^{3n-}$ layer. As shown in Figure 2, the difference is apparent when comparing the inorganic layer of **1** with that of **2**. Both layers of **1** and **2** contain $[Sn_6Se_{16}]$ chains along the *b* axis. In the structure of **1**, the $[Sn_3Se_7]_n^{2n-}$ layer is formed by the condensation of $[Sn_6Se_{16}]$ chains, thus leading to the generation of open windows constructed by six $[Sn_3Se_{10}]$ blocks in the layer. In the structure of **2**, the $[Sn_2Se_4(Se_2)(Se_6)_2]$ dimers are supposed to connect the $[Sn_6Se_{16}]$ chains to build up the $[Sn_4Se_8(Se_6)(Se_2)_{1/2}]_n^{3n-}$ layer, however, the windows constructed by six $[Sn_3Se_{10}]$ blocks and two $[Sn_2Se_4(Se_2)(Se_6)_2]$ dimmers are filled by Se_6^{2-} ions, which hinder the encapsulation of PEG chains within the structure.

By keeping all the reaction conditions the same as those used for **1**, and by increasing the reaction temperature to 140 °C, only a small amount of crystals of **1** was obtained. When the reaction temperature was upgraded to 160 °C, an orange emulsion, not crystals, can be obtained. When raising the reaction temperature to 190 °C, big red block crystals of **3** were isolated. The compound **3** crystallizes in the hexagonal space group *R*-3. Its structure features a two-dimensional anionic $[Sn_6Se_{14}]_n^{4n-}$ layer, which is charge balanced by $DBNH^+$ and NH_4^+. Notably, **3** is isostructural with **1** because of the structural similarity of the inorganic layers. However, no PEG chain was found in the structure of **3**. This difference can be attributed to their stacking arrangements. As illustrated in Figure 3, the inorganic layers of **1** are stacked in an AA sequence along the *c* axis, and the as-formed nanochannels are filled by PEG chains, while in the case of **3**, the inorganic layers are stacked in an ABCABC sequence along the *c* axis, and $DBNH^+$ cations are located in the center of nanochannels, consequently preventing the extended PEG chains from residing in the nanochannels.

Concluding from the syntheses of **1**–**3**, it is notable that reaction temperature plays an important role in synthesizing

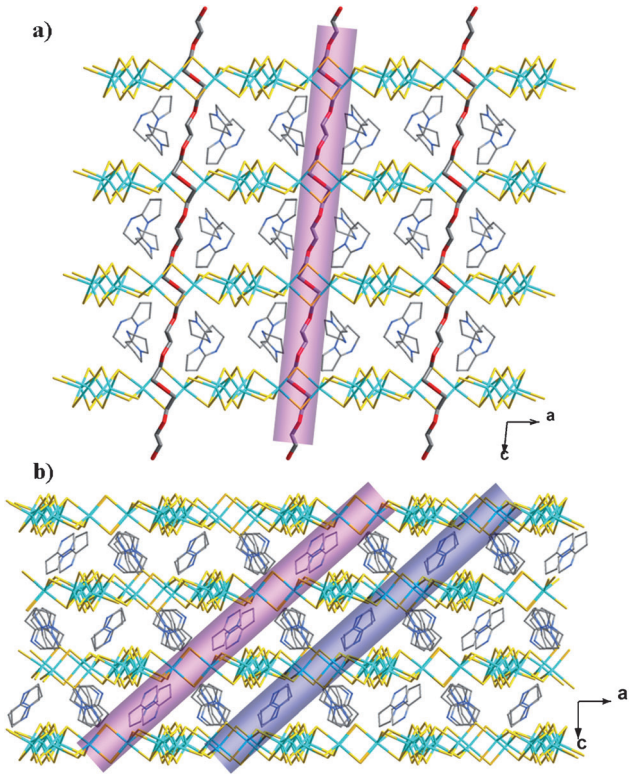

Figure 3. a) The inorganic layers of **1** are stacked in an AA sequence along the *c* axis, and the as-formed nanochannels are filled by PEG chains. b) The inorganic layers of **3** are stacked in an ABCABC sequence along the *c* axis, and the $DBNH^+$ cations are located in the center of nanochannels.

these compounds. It is well known that nonionic surfactants, such as polyoxyethylene, can be dissolved in H_2O or organic solvents because of the formation of hydrogen bonds between oxygen atoms from polyoxyethylene surfactants and H_2O or organic solvents. However, these hydrogen bonds can be destroyed by increasing the solution temperature, thus leading to the decrease of solubility of polyoxyethylene surfactants in H_2O or organic solvents. In the syntheses of **1**–**3**, when the reaction was run at 120 °C, PEG-400 can be mixed well with the solutions of H_2O and DBN, and the PEG chains interact with inorganic species and $DBNH^+$ cations through various C–H···Se and C–H···O hydrogen bonds, and was important for the construction of **1**. As the reaction temperature increased, the solubility of PEG-400 in the solutions of H_2O and DBN decreased, thus resulting in the crystals of **1** with a much lower yield at 140 °C, and only an emulsion formed at 160 °C. The disappearance of **2** may be ascribed to the unstable Se_6^{2-} ions at higher temperature. When the reaction was carried out at 190 °C, the solubility of PEG-400 in the solutions of H_2O and DBN was much lower, and then **3** without PEG chains was isolated under the reaction conditions.

The optical absorption spectra of **1**–**3** were converted from the solid-state UV-vis diffuse reflectance data by using the Kubelka-Munk function method. As shown in Figure 4 a, the sharp absorption edges suggest band gaps of 2.13 eV for **1**, 1.70 eV for **2**, 2.02 eV for **3**, which are consistent with their

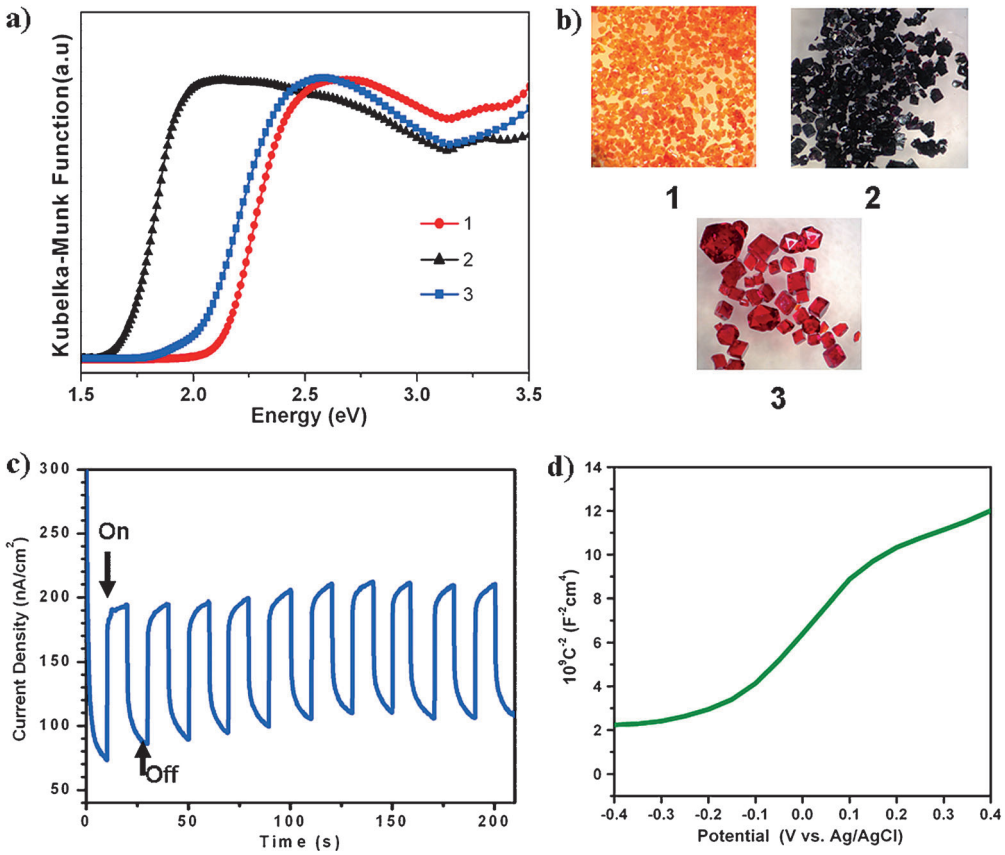

Figure 4. a) Solid-state optical absorption spectra of **1**–**3**. b) Photographs of the crystals of **1**–**3**. c) The photocurrent responses of a **1**/FTO photoelectrode with applied bias voltage (0.6 V vs. Ag/AgCl) upon chopped AM 1.5 G illumination. d) Mott-Schottky plot of **1** measured at a frequency of 1000 Hz.

colors. The thermogravimetric analysis (TGA) of **1** was performed under a N_2 atmosphere from 30 to 450 °C (see Figure S2 in the Supporting Information), and displayed a main weight loss of 26.9 % (theoretical value of 25.8 %) because of the loss per formula unit of two DBN molecules and one and a half PEG units.

The photoelectrochemical properties of **1** (a more detailed description is given in the Supporting Information) were studied in a photoelectrochemical cell with a three-electrode set-up. As shown in Figure 4 c, the anodic (positive) photocurrent responses of a **1**/FTO photoelectrode indicate that **1** exhibits n-type semiconductor characteristics under visible-light illumination ($\lambda > 400$ nm). By applying biased potential of 0.6 V, the photoelectrode can generate a photocurrent density of 110 nA/cm^2. The highly repeatable photocurrent profile suggests that **1** is very stable under illuminating conditions. The photocurrent-voltage (*J*-*V*) behavior of **1** was gathered by using linear sweep voltammetry in 0.5 M sodium sulfate solution (see Figure S3 in the Supporting Information). The photocurrent increases with increasing applied bias potential, and can generate a photocurrent density of 150 nA cm^{-2} at ~0.8 V (vs. Ag/AgCl). To further investigate the conductivity type and flat-band potential of **1**, Mott-Schottky measurement was performed in a 0.5 M sodium sulfate solution (pH 6.94). As shown in Figure 4 d, the positive slope of the linear region on the plot indicates that **1** is n-type conductive, which is consistent with the result in photoelectrochemical measurements. For estimating the flat-band potential of **1**, the measured voltage was converted into the reversible hydrogen electrode (RHE) scale by applying the following calculation: $V_{RHE} = V_{measured} + V^0_{Ag/AgCl} + 0.059 \times pH$, where V_{RHE} is the converted potential, $V_{measured}$ is the potential reading from potentiostat, and $V^0_{Ag/AgCl}$ is the potential difference between Ag/AgCl reference electrode and standard hydrogen electrode (SHE). Thus, the flat-band potential of this material is around 0.341 V versus RHE.

In summary, single crystals of the novel PEG/selenidostannate composite **1** have been produced by self-assembling inorganic hosts and PEG chains under surfactant-thermal conditions. The PEG chains occupy the nanochannels of the honeycomb $[Sn_3Se_7]_n^{2n-}$ layers and form various hydrogen bonds with $DBNH^+$ cations and $[Sn_3Se_7]_n^{2n-}$ anionic layers. Under the same reaction conditions, the isostructural compound **3** without a PEG chain was synthesized by increasing the reaction temperature to 190 °C. The synthesis procedure indicates that the hydrogen bonds formed between PEG chains and inorganic layers and $DBNH^+$ cations at lower temperature play an important role in self-assembling the PEG/selenidostannate composite **1**. Our success in preparing single crystals of polymer/chalcogenide composites could provide a new synthetic tool to encapsulate functional polymers within crystalline inorganic matrices for fundamental study and for device applications.

Experimental Section

Syntheses of $[DBNH]_2[Sn_3Se_7]\cdot PEG$ (**1**) and $[DBNH]_3[Sn_4Se_8(Se_6)(Se_2)_{1/2}]$ (**2**): 0.117 mg Sn (0.99 mmol), 0.194 mg Se (2.46 mmol), 1 mL DBN, 1 mL H_2O, 0.5 mL ethylene glycol, and 3 mL poly(ethylene glycol)-400 (PEG-400) were mixed and sealed into an autoclave equipped with a Teflon liner (23 mL), then heated at 120 °C for 6 days. After cooling to room temperature, the resulting products were washed with ethanol, and orange block crystals of **1** and black plate crystals of **2** were obtained in yields of 40.5 and 23.4 % (based on Sn), respectively.

Synthesis of $[DBNH]_3[NH_4][Sn_6Se_{14}]$ (**3**): All the reaction conditions were kept the same as those for **1** and **2**, except for an increase

of the reaction temperature to 190 °C. After cooling to room temperature, red block crystals of **3** were obtained by filtration and selected by hand (yield: 54.2 % based on Sn).

Crystallographic data for **1**: $C_{17}H_{32}N_4O_{1.5}Sn_3Se_7$, $M_r = 1225.26$, Monoclinic, $C2/c$, $a = 24.123(5)$ Å, $b = 13.590(3)$ Å, $c = 18.532(4)$ Å, $\beta = 95.65(3)°$ $V = 6046(2)$ Å^3, $Z = 8$. $2\theta_{max} = 55.02°$, $\rho_{calcd} = 2.692$ g cm^{-3}, $\mu = 10.909$ mm^{-1}, 6890 total reflections, 4928 observed ($I > 2\sigma(I)$), $R_1 = 0.0582$, $wR_2 = 0.1409$, GOF = 1.025.

Crystallographic data for **2**: $C_{21}H_{39}N_6Sn_4Se_{15}$, $M_r = 2034.74$, Monoclinic, $P2_1/c$, $a = 17.498(4)$ Å, $b = 13.767(3)$ Å, $c = 19.215(4)$ Å, $\beta = 98.81(3)°$ $V = 4574.1(16)$ Å^3, $Z = 4$. $2\theta_{max} = 54.96°$, $\rho_{calcd} = 2.955$ g cm^{-3}, $\mu = 14.121$ mm^{-1}, 10427 total reflections, 7848 observed ($I > 2\sigma(I)$), $R_1 = 0.0381$, $wR_2 = 0.0657$, GOF = 1.044.

Crystallographic data for **3**: $C_{21}H_{43}N_7Sn_6Se_{14}$, $M_r = 2211.20$, Hexagonal, R-3, $a = 27.651(4)$ Å, $c = 21.957(4)$ Å, $V = 14539(4)$ Å^3, $Z = 12$. $2\theta_{max} = 50.00°$, $\rho_{calcd} = 3.031$ g cm^{-3}, $\mu = 13.586$ mm^{-1}, 5670 total reflections, 5435 observed ($I > 2\sigma(I)$), $R_1 = 0.1297$, $wR_2 = 0.3195$, GOF = 1.011.

CCDC 1018680 (**1**), 1027199 (**2**), and 1027200 (**3**) contain the supplementary crystallographic data for this paper. These data can be obtained free of charge from The Cambridge Crystallographic Data Centre via www.ccdc.cam.ac.uk/data_request/cif.

Received: October 1, 2014
Published online: November 13, 2014

Keywords: electrochemistry · organic-inorganic hybrid composites · polymers · selenium · structure elucidation

[1] a) K. Moller, T. Bein, *Chem. Mater.* **1998**, *10*, 2950 – 2963; b) K. Tajima, T. Aida, *Chem. Commun.* **2000**, 2399 – 2412; c) D. J. Cardin, *Adv. Mater.* **2002**, *14*, 553 – 563.

[2] a) T. Bein, P. Enzel, *Angew. Chem. Int. Ed. Engl.* **1989**, *28*, 1692 – 1694; *Angew. Chem.* **1989**, *101*, 1737 – 1738; b) P. Enzel, T. Bein, *J. Phys. Chem.* **1989**, *93*, 6270 – 6272; c) K. Moller, T. Bein, R. X. Fischer, *Chem. Mater.* **1998**, *10*, 1841 – 1852; d) P. Uehara, H. Miyake, M. Matsuda, M. Sato, *J. Mater. Chem.* **1998**, *8*, 2133 – 2136; e) K. Kageyama, J. Tamazawa, T. Aida, *Science* **1999**, *285*, 2113 – 2115; f) P. Sozzani, S. Bracco, A. Comotti, R. Simonutti, P. Valsesia, Y. Sakamoto, O. Terasaki, *Nat. Mater.* **2006**, *5*, 545 – 551; g) T. Uemura, R. Kitaura, Y. Ohta, M. Nagaoka, S. Kitagawa, *Angew. Chem. Int. Ed.* **2006**, *45*, 4112 – 4116; *Angew. Chem.* **2006**, *118*, 4218 – 4222; h) T. Uemura, Y. Ono, Y. Hijikata, S. Kitagawa, *J. Am. Chem. Soc.* **2010**, *132*, 4917 – 4924; i) T. Uemura, N. Yanai, S. Watanabe, H. Tanaka, R. Numaguchi, M. T. Miyahara, Y. Ohta, M. Nagaoka, S. Kitagawa, *Nat. Commun.* **2010**, *1*, 83; j) T. Uemura, N. Uchida, A. Asano, A. Saeki, S. Seki, M. Tsujimoto, S. Isoda, S. Kitagawa, *J. Am. Chem. Soc.* **2012**, *134*, 8360 – 8363; k) G. Distefano, H. Suzuki, M. Tsujimoto, S. Isoda, S. Bracco, A. Comotti, P. Sozzani, T. Uemura, S. Kitagawa, *Nat. Chem.* **2013**, *5*, 335 – 341.

[3] a) T. Uemura, S. Horike, K. Kitagawa, M. Mizuno, K. Endo, S. Bracco, A. Comotti, P. Sozzani, M. Nagaoka, S. Kitagawa, *J. Am. Chem. Soc.* **2008**, *130*, 6781 – 6788; b) T. Uemura, Y. Ono, K. Kitagawa, S. Kitagawa, *Macromolecules* **2008**, *41*, 87 – 94.

[4] a) M. G. Kanatzidis, L. M. Tonge, T. J. Marks, H. O. Marcy, C. R. Kannewurf, *J. Am. Chem. Soc.* **1987**, *109*, 3797 – 3799; b) M. G. Kanatzidis, C. G. Wu, H. O. Marcy, C. R. Kannewurf, *J. Am. Chem. Soc.* **1989**, *111*, 4139 – 4141; c) R. Bissessur, D. C. Degroot, J. L. Schindler, C. R. Kannewurf, M. G. Kanatzidis, *J. Chem. Soc. Chem. Commun.* **1993**, 687 – 689; d) Y. J. Liu, D. C. Degroot, J. L. Schindler, C. R. Kannewurf, M. G. Kanatzidis, *Adv. Mater.* **1993**, *5*, 369 – 372; e) Y. J. Liu, D. C. Degroot, J. L. Schindler, C. R. Kannewurf, M. G. Kanatzidis, *J. Chem. Soc. Chem. Commun.* **1993**, 593 – 596.

[5] a) P. Sozzani, R. W. Behling, F. C. Schilling, S. Bruckner, E. Helfand, F. A. Bovey, L. W. Jelinski, *Macromolecules* **1989**, *22*, 3318 – 3322; b) P. Sozzani, F. A. Bovey, F. C. Schilling, *Macromolecules* **1991**, *24*, 6764 – 6768; c) F. C. Schilling, K. R. Amundson, P. Sozzani, *Macromolecules* **1994**, *27*, 6498 – 6502; d) M. Farina, G. Di Silvestro, P. Sozzani, *Comprehensive Supramolecular Chemistry*, *Vol. 6* (Ed.: J.-M. Lehn), Pergamon, Oxford, **1996**; e) P. Sozzani, A. Comotti, S. Bracco, R. Simonutti, *Chem. Commun.* **2004**, 768 – 769; f) A. Comotti, S. Bracco, T. Ben, S. L. Qiu, P. Sozzani, *Angew. Chem. Int. Ed.* **2014**, *53*, 1043 – 1047; *Angew. Chem.* **2014**, *126*, 1061 – 1065.

[6] a) O. M. Yaghi, Z. Sun, D. A. Richardson, T. L. Groy, *J. Am. Chem. Soc.* **1994**, *116*, 807 – 808; b) H. L. Li, A. Laine, M. O'Keeffe, O. M. Yaghi, *Science* **1999**, *283*, 1145 – 1147; c) N. F. Zheng, X. H. Bu, P. Y. Feng, *Nature* **2003**, *426*, 428 – 432; d) P. Y. Feng, X. H. Bu, N. F. Zheng, *Acc. Chem. Res.* **2005**, *38*, 293 – 303; e) S. Dehnen, M. Melullis, *Coord. Chem. Rev.* **2007**, *251*, 1259 – 1280; f) M. L. Feng, D. N. Kong, Z. L. Xie, X. Y. Huang, *Angew. Chem. Int. Ed.* **2008**, *47*, 8623 – 8626; *Angew. Chem.* **2008**, *120*, 8751 – 8754; g) Q. Zhang, Y. Liu, X. H. Bu, T. Wu, P. Y. Feng, *Angew. Chem. Int. Ed.* **2008**, *47*, 113 – 116; *Angew. Chem.* **2008**, *120*, 119 – 122; h) M. J. Manos, M. G. Kanatzidis, *J. Am. Chem. Soc.* **2009**, *131*, 6599 – 6607; i) Q. Zhang, I. Chung, J. I. Jang, J. B. Ketterson, M. G. Kanatzidis, *J. Am. Chem. Soc.* **2009**, *131*, 9896 – 9897; j) J. Zhou, J. Dai, G. Q. Bian, C. Y. Li, *Coord. Chem. Rev.* **2009**, *253*, 1221 – 1247; k) M. G. Kanatzidis, N. Ding, *Nat. Chem.* **2010**, *2*, 187 – 191; l) W. Xiong, G. Zhang, Q. Zhang, *Inorg. Chem. Frontiers* **2014**, *1*, 292 – 304.

[7] a) M. J. MacLachlan, N. Coombs, G. A. Ozin, *Nature* **1999**, *397*, 681 – 684; b) P. N. Trikalitis, K. K. Rangan, T. Bakas, M. G. Kanatzidis, *Nature* **2001**, *410*, 671 – 675; c) Q. Zhang, X. Bu, L. Han, P. Feng, *Inorg. Chem.* **2006**, *45*, 6684 – 6687; d) S. Bag, P. N. Trikalitis, P. J. Chupas, G. S. Armatas, M. G. Kanatzidis, *Science* **2007**, *317*, 490 – 493; e) T. Wu, X. Q. Wang, X. H. Bu, X. Zhao, L. Wang, P. Y. Feng, *Angew. Chem. Int. Ed.* **2009**, *48*, 7204 – 7207; *Angew. Chem.* **2009**, *121*, 7340 – 7343; f) Q. Zhang, G. Armatas, M. G. Kanatzidis, *Inorg. Chem.* **2009**, *48*, 8665 – 8667; g) Q. Zhang, C. D. Malliakas, M. G. Kanatzidis, *Inorg. Chem.* **2009**, *48*, 10910 – 10912; h) S. Bag, M. G. Kanatzidis, *J. Am. Chem. Soc.* **2010**, *132*, 14951 – 14959; i) J. R. Li, Z. L. Xie, X. W. He, L. H. Li, X. Y. Huang, *Angew. Chem. Int. Ed.* **2011**, *50*, 11395 – 11399; *Angew. Chem.* **2011**, *123*, 11597 – 11601; j) Y. M. Lin, W. Massa, S. Dehnen, *J. Am. Chem. Soc.* **2012**, *134*, 4497 – 4500.

[8] a) R. Bissessur, M. G. Kanatzidis, J. L. Schindler, C. R. Kannewurf, *J. Chem. Soc. Chem. Commun.* **1993**, 1582 – 1585; b) M. G. Kanatzidis, R. Bissessur, D. C. Degroot, J. L. Schindler, C. R. Kannewurf, *Chem. Mater.* **1993**, *5*, 595 – 596.

[9] a) W. W. Xiong, E. U. Athresh, Y. T. Ng, J. F. Ding, T. Wu, Q. Zhang, *J. Am. Chem. Soc.* **2013**, *135*, 1256 – 1259; b) W. W. Xiong, P. Z. Li, T. H. Zhou, A. L. Y. Tok, R. Xu, Y. L. Zhao, Q. Zhang, *Inorg. Chem.* **2013**, *52*, 4148 – 4150; c) J. K. Gao, Q. L. Tay, P. Z. Li, W. W. Xiong, Y. L. Zhao, Z. Chen, Q. Zhang, *Chem. Asian J.* **2014**, *9*, 131 – 134; d) G. Zhang, P. Li, J. Ding, Y. Liu, W. Xiong, L. Nie, T. Wu, Y. Zhao, A. I. Y. Tok, Q. Zhang, *Inorg. Chem.* **2014**, *53*, 10248 – 10256.

[10] a) T. Jiang, A. Lough, G. A. Ozin, *Adv. Mater.* **1998**, *10*, 42 – 46; b) T. Jiang, G. A. Ozin, *J. Mater. Chem.* **1998**, *8*, 1099 – 1108; c) A. Fehlker, R. Blachnik, *Z. Anorg. Allg. Chem.* **2001**, *627*, 1128 – 1134; d) J. R. Li, W. W. Xiong, Z. L. Xie, C. F. Du, G. D. Zou, X. Y. Huang, *Chem. Commun.* **2013**, *49*, 181 – 183; e) Y. M. Lin, D. W. Xie, W. Massa, L. Mayrhofer, S. Lippert, B. Ewers, A. Chernikov, M. Koch, S. Dehnen, *Chem. Eur. J.* **2013**, *19*, 8806 – 8813.

